URSI GASS 2021, Rome, Italy, 28 August - 4 September 2021

SAR Target Configuration Recognition Based on Integrated Graph Model

Ming Liu* (1) and Shichao Chen(2)
(1) School of Computer Science, Shaanxi Normal University, Xi'an 710119, China
(2) No. 203 Research Institute of China Ordnance Industries, Xi'an 710065, China

Abstract

Focusing on the problem of target configuration recognition in synthetic aperture radar (SAR) images, a recognition method using an integrated graph model (IGM) is proposed in this paper. The information of the samples is preserved in different views. To achieve stronger discriminative power, a modified sparse graph employing sign correction of the sparse coefficients is proposed to describe the relationships of the samples. Furthermore, to realize more complete information capturing, the classical Euclidean distance-based affinity matrix together with the proposed modified sparse graph are fused to achieve an integrated graph. Experimental results on the moving and stationary target acquisition and recognition (MSTAR) datasets verify the effectiveness of the proposed method. Satisfying configuration recognition results can be obtained by using the proposed methods.

1 Introduction

One of the hottest research topics of synthetic aperture radar (SAR) applications is automatic target recognition (ATR) [1-3]. It plays a crucial role in plenty of application areas, such as environment monitoring, disaster evaluation, foe and friend identification, and precise attack [1-3]. As a result, SAR ATR has attracted increasing interests nowadays.

Manifold learning aims to find the intrinsic structure characteristics of the datasets in the manifold space, which can give a better description of the datasets. Therefore, taking the manifold structure of the datasets into consideration results in better feature extraction. Based on the idea of manifold learning, several algorithms have been proposed to deal with the problem of SAR ATR. Huang et al. proposed a neighborhood geometric center scaling embedding (NGCSE) algorithm [4], which improves the recognition rates of SAR targets effectively. Liu et al. proposed a sample discriminant analysis (SDA) algorithm which is an image-based dimensionality reduction method. SAR images no longer need to be transformed into columns by using the SDA algorithm [5]. Taking the statistical property of the SAR images into account, Liu et al. proposed a recognition algorithm that combines the locality property of the samples and the Gaussian mixture distribution of SAR images [6]. Besides, an algorithm that fuses a more appropriate Gamma distribution and the locality property of the samples is proposed to further enhance the recognition performance [7].

One of the key points of the manifold learning-based algorithms is to describe the relationships of the samples by the constructed graph. However, the relationships of the samples are only described by the Euclidean distance in the algorithms mentioned above. As a result, the effectiveness of the recognition algorithms is still limited. As is known, SAR images suffer from target aspect angle sensitivity. Differences among the samples belong to different types but with similar target aspect angles are much smaller than those belong to the same type but with explicit different target aspect angles. Detail discussions can be found in literatures [3, 7]. The phenomenon leads to great difficulties for effective feature extraction and recognition for SAR ATR. Focusing on the problem, a modified sparse graph is constructed to establish the relationships of the samples in this paper. And more sufficient information is captured and preserved by fusing multiple graphs to an integrated graph. The local structure of the SAR images can be described in a much better way. Thanks to the great local structure capturing and preserving power, the proposed method is capable of recognizing target samples not only belong to different target types, but also belong to different target configurations. Configurations are samples belong to the same target type, but with tiny differences [3, 6-7].

2 The proposed Integrated Graph Model based recognition algorithm

Local structure has been proved to be of great importance to pattern recognition, and locality preserving projections (LPP) can realize local structure preserving by constructing the following objective function [8]

$$\arg\min \sum_{i,j} \left\| \mathbf{y}_i - \mathbf{y}_j \right\|_2^2 \mathbf{S}_{ij} \tag{1}$$

where $\mathbf{y}_i = \mathbf{A}^T \mathbf{x}_i$, $\mathbf{X} = \{\mathbf{x}_1, \mathbf{x}_2, ..., \mathbf{x}_n\}$ represents the samples in the high-dimensional space, $\mathbf{Y} = \{\mathbf{y}_1, \mathbf{y}_2, ..., \mathbf{y}_n\}$ is the samples in the low-dimensional space, n is the number of the samples in the training datasets, $\mathbf{A}$ is the projection matrix, $\|\bullet\|_2$ denotes the L2 norm, the symbol ^{T} represents the matrix transpose and

$\mathbf{S}$ is the affinity matrix that describes the relationships of the samples.

One of the key steps of LPP is the construction of the affinity matrix. Different affinity matrices can capture and preserve the structure of the samples in different views. As discussed previously, we try to realize structure capturing and preserving of the datasets by fusing multiple graph models together. More powerful information can be preserved and captured by the integrated graph, and more useful information will result in better recognition results.

In this paper, we give two different ways of constructing the affinity matrices, then we fuse them together. The weights of the graphs can be adjusted by the fusion coefficients. In the first way, the affinity matrix $\mathbf{S}$ is constructed based on the Euclidean distance [8]

$$\mathbf{S}_{ij} = \begin{cases} \exp\left(-\dfrac{\left\|\mathbf{x}_i - \mathbf{x}_j\right\|_2}{t}\right) & class\left(\mathbf{x}_i\right) = class\left(\mathbf{x}_j\right) \\ 0 & class\left(\mathbf{x}_i\right) \neq class\left(\mathbf{x}_j\right) \end{cases} \tag{2}$$

where t is a constant. (2) describes the relationships of the samples in the following way: if $\mathbf{x}_i$ and $\mathbf{x}_j$ belong to the same class, the weight calculated by (2) will be imposed on $\mathbf{x}_i$ and $\mathbf{x}_j$. Otherwise, the relationship of them will not be established to avoid disturbances.

In the second way, we constructed the affinity matrix based on the sparse graph [9]. The objective function of sparse representation (SR) can be described as [10]

$$\min \left\|\boldsymbol{\alpha}_i\right\|_0 \quad s.t.\ \mathbf{x}_i = \mathbf{X}\boldsymbol{\alpha}_i \tag{3}$$

where $\boldsymbol{\alpha}_i$ is the sparse vector of $\mathbf{x}_i$, and $\left\|\bullet\right\|_0$ denotes the L0 norm. The sparse vectors can be calculated by using the basis pursuit (BP) algorithm [11] or the orthogonal matching pursuit (OMP) algorithm [12]. Base on the sparse vectors, we construct the affinity matrix $\mathbf{W}$ by [9]

$$\mathbf{W} = \frac{\boldsymbol{\Phi} + \boldsymbol{\Phi}^T}{2} \tag{4}$$

where $\boldsymbol{\Phi} = \left\{\boldsymbol{\alpha}_1, \boldsymbol{\alpha}_2, ..., \boldsymbol{\alpha}_n\right\}$. Here, we give a brief discussion on this point. The sparse vectors $\boldsymbol{\alpha}_i \left(i = 1, 2, ..., n\right)$ contain the discriminative power together with structure information of the samples. As a result, the affinity matrix $\mathbf{W}$ constructed based on the sparse vectors contains not only the structure information of the samples, but also the discriminative power.

In this paper, to enhance the recognition performance, we propose a modified sparse graph. Having the sparse vector $\boldsymbol{\alpha}_i$ in hand, we will judge the plus or minus sign for each entry. If the sample of the entry has the same label with the sample $\mathbf{x}_i$, we will impose a plus sign on the entry. Otherwise, we will impose a minus sign on it if its label is different from the sample $\mathbf{x}_i$. Taking a BMP2-9563 sample as an illustration, Figure 1 shows the sparse vector of a BMP2-9563 sample and Figure 2 displays the modified version. From Figure 1, we can see that the nonzero entries of the sparse vector not only lie in the positions that correspond to configuration BMP2-9563, but also lie in positions that correspond to different configurations because of the target aspect angle sensitivity of SAR images. Due to the existence of these nonzero entries that correspond to different configurations, samples belong to different configurations will become closer when minimizing (1). This will lead to poor recognition results. So as to ease the problem, the signs of the nonzero entries correspond to the samples with different configurations but with plus sign are changed to minus. Then the distance among the samples belong to different configurations can be enlarged in the low-dimensional space when minimizing (1). Likewise, for the negative entries within the same configuration, minimizing the objective function will enlarge the distance of the samples. Changing the sign of these entries will contribute to distance shrinking of the samples with the same configurations but with the minus sign in the low-dimensional space. Discriminative power of the sparse graph can be further enhanced by using the proposed sign correction method.

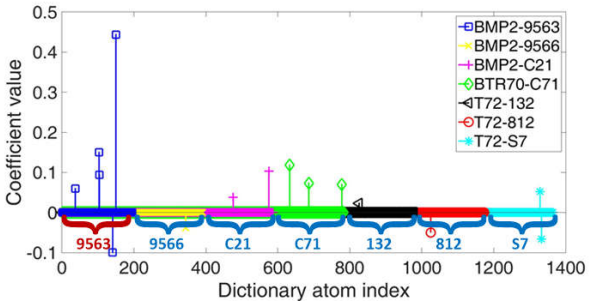

Figure 1. The sparse vector of a BMP2-9563 sample.

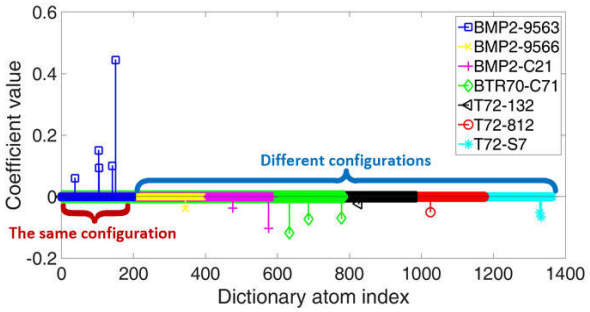

Figure 2. The modified sparse vector of a BMP2-9563 sample.

In order to fuse the advantages of the two graph models, the integrated graph $\mathbf{G}$ can be obtained by

$$\mathbf{G} = k\mathbf{S} + (1-k)\mathbf{W} \tag{5}$$

where k represents the fusion coefficient that can balance the weights of the graph models.

Replacing the affinity matrix $\mathbf{S}$ in (1) with $\mathbf{G}$ in (5), we can have the following equation

$$\mathbf{X}\mathbf{L}\mathbf{X}^T\mathbf{A} = \lambda\mathbf{X}\mathbf{D}\mathbf{X}^T\mathbf{A} \tag{6}$$

where $\mathbf{D}$ is a diagonal matrix whose entries $\mathbf{D}_{ii} = \sum_j \mathbf{G}_{ij}$ are the column sum of $\mathbf{G}$, and $\mathbf{L} = \mathbf{D} - \mathbf{G}$.

The projection matrix $\mathbf{A}$ can be obtained by solving the generalized eigen decomposition problem expressed as (6). Then the training datasets and the testing datasets can be projected onto the low-dimensional space by using $\mathbf{A}$. Finally, a k-nearest neighbor (k-NN) classifier is adopted to achieve recognition.

3 Experimental Results and Analysis

Experiments on the moving and stationary target acquisition and recognition (MSTAR) datasets are conducted to test the effectiveness of the proposed method. SAR images collected with the depression angles 15° are used as the training samples, whereas SAR images collected with the depression angle 17° are used as the testing samples. All the original images are 128×128 pixels, and the redundant background is excluded to get a 48×48 pixels sub-image from the center of each image. The sizes of the training and testing datasets are given in Table 1.

Table 1. Experimental datasets.

Type	BMP2			BTR70	T72			Sum
Configuration	9563	9566	C21	C71	132	812	S7	
Training (15°)	195	196	196	196	196	195	191	1365
Testing (17°)	233	232	233	233	232	231	228	1622

Recognition results under these algorithms are displayed in Table 2. Here, LPP-IGM represents the proposed integrated graph model-based algorithm. The principal component analysis (PCA) based algorithm [8], the LPP based algorithm using the Euclidean distance to establish the affinity matrix (LPP-ED) [8], the LPP based algorithm using the sparse graph to establish the affinity matrix (LPP-SG) [9], and the LPP based algorithm using the modified sparse graph to establish the affinity matrix (LPP-MSG) are taken as competitors to show the advantage of the proposed method. And the dimensionality of all the algorithms are set to be 120. The fusion coefficient k is determined by the 5-fold cross validation from the set $[0.2, 0.4, 0.6, 0.8]$.

As can be seen from Table 2, the traditional PCA based method can only realize the accurate recognition rate of 70.59%. Due to the structure preserving ability of LPP, both LPP-SG and LPP-ED can achieve much better performance. The recognition rates can reach 87.85% and 89.77%, respectively. The results have further verified the importance of local structure preserving to recognition. LPP-MSG can obtain higher recognition rates than LPP-SG due to the modification of the sparse graph. Thanks to the integrated graph model, which fuses both the advantage of LPP-MSG and LPP-ED, LPP-IGM can achieve better recognition results with respect to the single graph model-based algorithms (LPP-MSG, LPP-SG and LPP-ED). The proposed LPP-IGM method can get the highest recognition rate of 90.01%, which is 0.06%, 2.16%, 0.24%, 19.42% better than LPP-MSG, LPP-SG, LPP-ED and PCA, respectively. Corresponding confusion matrix of the proposed LPP-IGM method is demonstrated in Table 3.

Table 2. Configuration recognition results.

Method	Recognition rate
LPP-IGM (%)	90.01
LPP-MSG (%)	89.95
LPP-SG (%)	87.85
LPP-ED (%)	89.77
PCA (%)	70.59

Table 3. Confusion matrix of the proposed LPP-IGM algorithm.

	BMP2 9563	BMP2 9566	BMP2 C21	BTR70 C71	T72 132	T72 812	T72 S7
BMP2 9563	184	17	32	0	0	0	0
BMP2 9566	25	198	8	1	0	0	0
BMP2 C21	23	11	199	0	0	0	0
BTR70 C71	0	1	0	232	0	0	0
T72 132	0	0	0	0	229	3	0
T72 812	0	0	0	0	0	212	19
T72 S7	0	0	0	0	11	11	206

4 Conclusion

An integrated graph model is proposed to realize better description of the datasets in this paper. Satisfying recognition results are obtained due to the more complete structure capturing and preserving of the datasets. More than 90% accurate recognition rates for SAR target configuration recognition can be obtained by using the proposed integrated graph model-based method.

However, we just fuse two different graph models in this paper. To achieve even better recognition results, we can fuse more graph models to capture and preserve the intrinsic structure of the datasets from different views.

5 Acknowledgements

This research was funded by the National Natural Science Foundation of China, grant number 61701289, the Young Talent Fund of University Association for Science and Technology in Shaanxi, grant number 20190106, the Fundamental Research Funds for the Central Universities grant number GK202103088, and the Special Support Program for High Level Talents of Shaanxi Province.

6 References

1. L. Chen, X. Jiang, Z. Li, X. Liu, and Z. Zhou, "Feature-Enhanced Speckle Reduction via Low-Rank and Space-Angle Continuity for Circular SAR Target Recognition," *IEEE Transactions on Geoscience and Remote Sensing*, **58**, 11, November 2020, pp. 7734-7752, doi: 10.1109/TGRS.2020.2983420.

2. J. Wang, J. Liu, P. Ren, and C. -X. Qin, "A SAR Target Recognition Based on Guided Reconstruction and Weighted Norm-Constrained Deep Belief Network," *IEEE Access*, **8**, 2020, pp. 181712-181722, doi: 10.1109/ACCESS.2020.3025379.

3. M. Liu, S. Chen, J. Wu, F. Lu, X. Wang, and M. Xing, "SAR Target Configuration Recognition via Two-Stage Sparse Structure Representation," *IEEE Transactions on Geoscience and Remote Sensing*, **56**, 4, April 2018, pp. 2220-2232, doi: 10.1109/TGRS.2017.2776600.

4. Y. Huang, J. Pei, J. Yang, B. Wang, and X. Liu, "Neighborhood Geometric Center Scaling Embedding for SAR ATR," *IEEE Transactions on Aerospace and Electronic Systems*, **50**, 1, January 2014, pp. 180-192, doi: 10.1109/TAES.2013.110769.

5. X. Liu, Y. Huang, J. Pei, and J. Yang, "Sample Discriminant Analysis for SAR ATR," *IEEE Geoscience and Remote Sensing Letters*, **11**, 12, December 2014, pp. 2120-2124, doi: 10.1109/LGRS.2014.2321164.

6. M. Liu, Y. Wu, P. Zhang, Q. Zhang, Y. Li, and M. Li, "SAR Target Configuration Recognition Using Locality Preserving Property and Gaussian Mixture Distribution," *IEEE Geoscience and Remote Sensing Letters*, **10**, 2, March 2013, pp. 268-272, doi: 10.1109/LGRS.2012.2198610.

7. M. Liu, Y. Wu, Q. Zhang, F. Wang, and M. Li, "Synthetic Aperture Radar Target Configuration Recognition Using Locality-Preserving Property and the Gamma Distribution," *IET Radar, Sonar & Navigation*, **10**, 2, February 2016, pp. 256-263, doi: 10.1049/iet-rsn.2015.0024.

8. X. He, S. Yan, Y. Hu, P. Niyogi, and H. Zhang, "Face Recognition Using Laplacianfaces," *IEEE Transactions on Pattern Analysis and Machine Intelligence*, **27**, 3, March 2005, pp. 328-340, doi: 10.1109/TPAMI.2005.55.

9. M. Liu, S. Chen, F. Lu, J. Wang, J. Wu, and T. Yang, "Achieving SAR Target Configuration Recognition By Combining Sparse Graph And Locality Preserving Projections," *2018 IEEE International Geoscience and Remote Sensing Symposium*, Valencia, 2018, pp. 29-32, doi: 10.1109/IGARSS.2018.8519157.

10. J. Wright, A. Y. Yang, A. Ganesh, S. S. Sastry, and Y. Ma, "Robust Face Recognition via Sparse Representation," *IEEE Transactions on Pattern Analysis and Machine Intelligence*, **31**, 2, February 2009, pp. 210-227, doi: 10.1109/TPAMI.2008.79.

11. S. Chen, D. Donoho, and M. Saunders, "Atomic Decomposition by Basis Pursuit," *SIAM Review*, **43**, 1, 2001, pp. 129–159. doi: 10.1137/S003614450037906X.

12. J. A. Tropp and A. C. Gilbert, "Signal Recovery From Random Measurements Via Orthogonal Matching Pursuit," *IEEE Transactions on Information Theory*, **53**, 12, December 2007, pp. 4655-4666, doi: 10.1109/TIT.2007.909108.